Satellite-based Flooded Area and Depth Prediction

Siripon Kamontum, Anusorn Rungsipanich,
Kampanat Deeudomchan, Thudchai Sansena and Siam Lawawirojwong
Geo-informatics and Space Technology Development Agency (GISTDA)
120 Moo 3 Building B, 6th & 7th Floors, Chaeng Wattana Rd., Lak Si
Bangkok 10210, THAILAND
Fax (+66) 0-2143-9594 E-mail: siripon@gistda.or.th

Abstract

Flood is one of serious disasters causing social-economic losses. The government and people in the susceptible areas have concerned on necessity of flood prediction for flood response planning.

An objective of this study is to develop a method for flood prediction using high resolution DEM, hydrological data and satellite images, which will be utilized as a foundation to answer flood related questions, such as will a certain area be flooded, when, and how deep is the flood water. The study area is Phra Nakhon Si Ayutthaya and Pathum Tani provinces, Thailand that has various land uses, for instance, agricultural, urban, archeological and industrial areas, which have been damaged by the previous floods.

In this study, we identified relationship between water level (measured at gauge stations) and inundated areas (interpreted from the satellite images) during 2006 to 2014. For flooded area prediction, the predicted water level was used as the input and plugged in to the identified relationship, and the predicted flooded areas were then calculated. We overlaid the predicted flooded areas on the high resolution DEM to produce flood depth maps. The maps portraying predicted flooded areas with water depth can be produced on a daily basis, 3 days in advance. The flood prediction maps were compared to in situ data for accuracy assessment. The advantage of the proposed method is fast, simple, and suitable to use during a flood disaster and the result is operational used at GISTDA. Also, these maps can be used as an input for flood response planning.

Key words: flood, satellite images, Phra Nakhon Si Ayutthaya

1. Introduction

One of serious disasters causing socio-economic losses is flooding. In Thailand, people in the flood prone areas and the government concern on the hazard and require a flood model to predict the situation in advance, so they can prepare for it appropriately.

In Thailand, departments having mandate in water resource management, such as the Royal Irrigation Department, established stream gauge stations along the rivers and developed models to predict water level at location of the main gauges. These predicted water levels are useful for over bank flood prediction. However, the predicted water levels are available at the gauge locations only. If a method to extrapolate the predicted water level to cover the vicinity flood plain was developed, information of the predicted flood situation on the flood plain could be derived and would be useful for people susceptible to the flood, and they could prepare for it accordingly.

To estimate level of the flood water on the flood plain, using only predicted water level at the gauge stations was not enough because there were other factors controlling the flood such as topography and human activities. As a result, topographic data were required in this study. For human activities in flood controlling, satellite images were used to characterize historical flood pattern. An objective of this study was to develop a method for flood prediction using high resolution DEM, hydrological data measured at stream gauges and satellite images.

Satellite images were generally used in flood delineation such as a study of Marti-Cardona et al. (2010), which flood movement in Donna wetland, Spain was monitored using ASAR/Envisat HH and VV polarization data. Also, Pulvirenti et al. (2011) used COSMO-SkyMed spotlight mode data to monitor flood movement in northern Italy. To reassure the utilization of satellite images in flood delineation, Schumann et al. (2011) assessed accuracy of using TerraSAR-X images for flood boundary extraction comparing to aerial photos. Other than flood boundary, level of flood water could be extracted using satellite images as stated in a study of Mason et al. (2012) that TerraSAR-X images and control points with topographic elevation data were used to calculate level of the flood water. Furthermore, level of flood water on a flood plain of lower Amazon basin was derived from data measured at the river gauge using regression analysis to establish relationship between flooded areas interpreted from ALOS/PULSAR ScanSAR images and water level measured at the gauge (Arnesen et al., 2013).

2. Methodology

2.1 Study Area

The study area was an 865 SqKm floodplain in lower Chao Phraya river basin covering parts of Phranakhon Si Ayutthaya and Pathum Tani provinces, which has 3 stream gauge stations including C.35, C.29 and S.5, as illustrated in Figure 1.

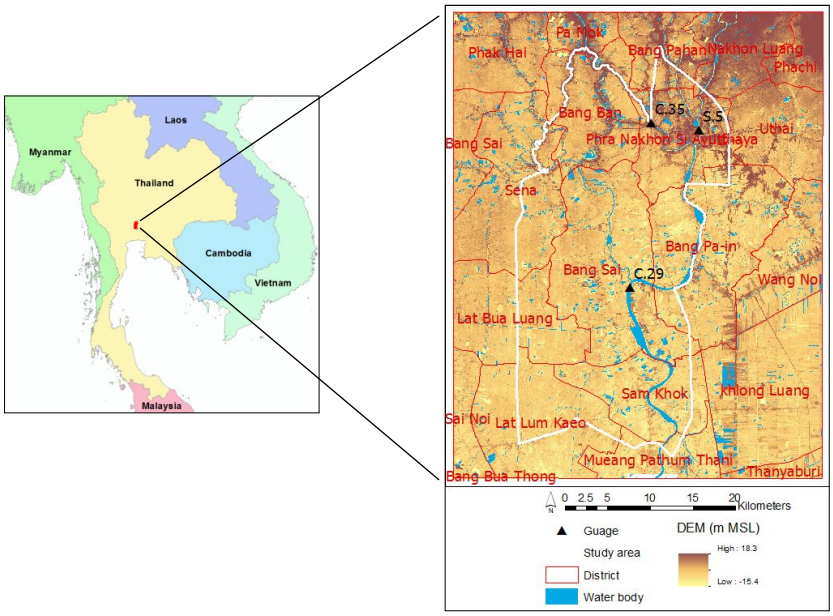

Figure 1 Study area

2.2 Data

2.2.1 Water Level

At 3 gauging stations (C.35, S.5 and C.29) in the study area, predicted water levels, 3 days in advance, are published via the web site of the Royal Irrigation Department (http://floodinfo.rid.go.th/) during the critical period. These predicted data were inputs of the developed flood model. These water level data were later matched with the satellite images to form a relationship between water levels measured at the gauges and flooded areas in the flood plain.

2.2.2 Flooded Areas

Flooded areas were interpreted from 71 satellite images of Radarsat 1 and 2, Alos 1, Landsat 5, and Thaichote acquired during 2006-2012. An example of Radarsat 2 image used in this study is shown in Figure 2. This study focused on overbank flood, which water level measured at a gauge describes flood situation in the neighboring flood plain, but for 2011 large flood, it was not

overbank flood. For this reason, all satellite images acquired in 2011 were eliminated, and only 34 images were left for the flood model development. Interpreted from the 34 images, flooded areas were stored in ESRI shape file format for flood model development later.

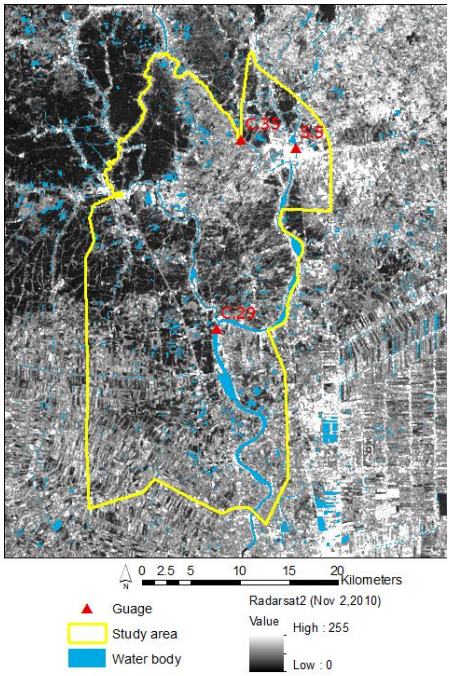

Figure 2 Radarsat 2 image acquired on November 2, 2010

2.2.3 LiDAR DEM

In this study, we used 30 cm vertical accuracy with 2 m pixel size LiDAR DEM to describe topographic variation of the area. Elevation value of the DEM changes 10 cm at a time. Levees, ridges, and roads appearing as dark tone linear structures could be distinguished in the DEM, as shown in Figure 3.

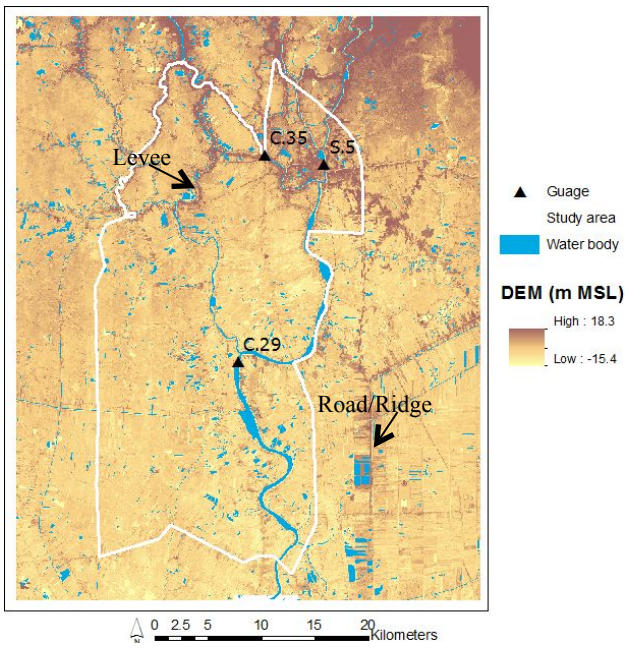

Figure 3 LiDAR DEM with 30 cm vertical accuracy

2.3 Flood Model Development Using Look up Table Concept

Flowchart of flood model development using look up table (LUT) concept was illustrated in Figure 4. The process included delineation of influence areas of the gauge stations, matching between flooded areas and water levels, water level interpolation, flood water depth calculation, and LUT creation.

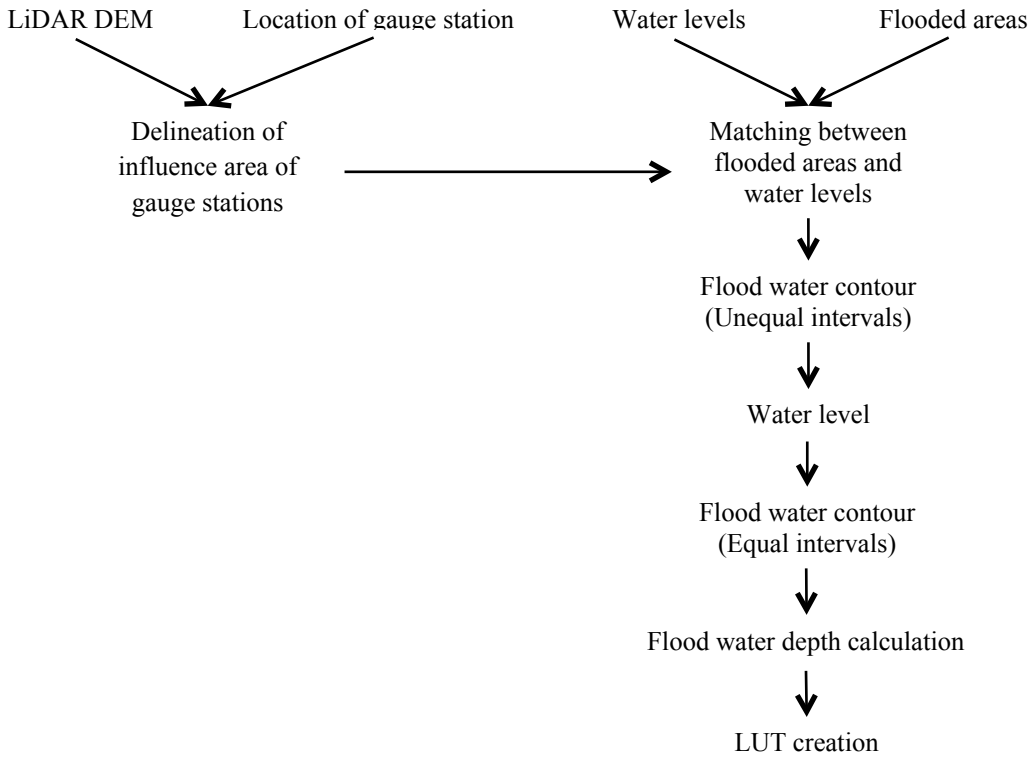

Figure 4 Flowchart of flood model development

2.3.1 Delineation of Influence Areas of the Gauge Stations

Water level data used in this study were measured at 3 gauge stations including C.35, S.5, and C.29. A water level measured at a station described flood situation in a specific area. Therefore, influence area of each station had to be defined. Roughly, we defined influence area of each station using Theissen polygons, where the centroids were the gauge locations. However, in the real world, topography controls flood water propagation. As a result, we used the LiDAR DEM to divide the study area into small catchment areas, called pond cells, which their borders were levee, road, or ridge, for example. Next, we combined the pond cells to the Theissen polygons, and then the influence area of each gauge station was defined, as shown in Figure 5. The influence area was a group of pond cells that majority of their body were in the same Theissen polygon, and flood situation in these pond cells was under influence of water level measure at the gauge station locating at centroid of this Theissen polygon.

According to Figure 5, gauge C.29 has the largest influence area covering central and southern parts of the study area, while C.35 and S.5 have smaller influence areas locating in northern part of study area. To study impact of water levels (measured at the gauges) on flood situations, the analysis was carried out base on these influence areas.

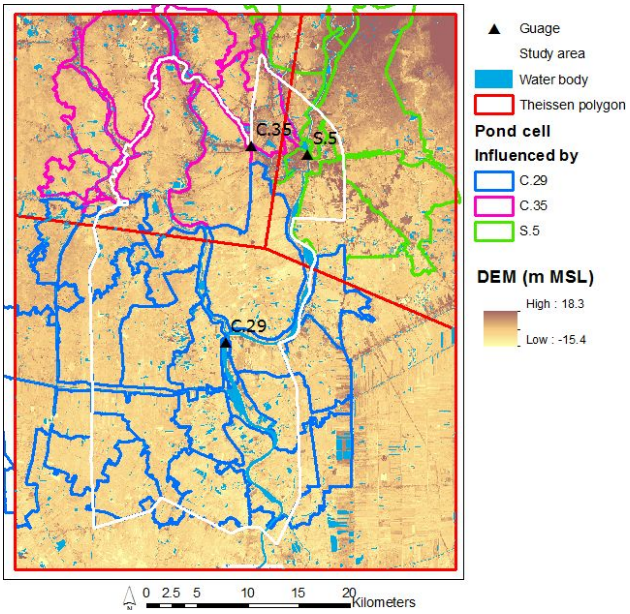

Figure 5 Influence areas of the gauge stations

Height of the river bank is another important factor controlling the overbank flood. The lowest point of the river bank is a location where the water spreads from the river into the flood plain. In a certain influence area, if a water level measured at the gauge or input into the model by a user is lower than the lowest point of the river bank, the situation is deemed no flood.

For each influence area, the lowest point of the river bank was identified using the LiDAR DEM by comparing between the lowest points of left and right banks, and the minimum value was considered the lowest bank elevation where overbank flood starts spreading. In this study, the minimum bank elevation was used because the study area is flat, and heights of left and right banks are very similar.

2.3.2 Matching between Flooded Areas and Water Levels

To create the LUT based on historical data, we matched flooded areas (interpreted from the satellite images) with water level (measured at the gauge stations). Later, LUT was used to predict flooded areas by inputting a predicted water level, and output was a layer of flooded areas estimated based on historical data.

Generally, water level data are available daily, but satellite data are available only on the acquisition date. As a result, matching between flooded areas and water level could not be done on a daily basis. Furthermore, for overbank flood, high water level at a gauge causes flooding in the neighboring flood plain day(s) later because flood water needs time for propagation. Therefore, we could not match flooded areas (interpreted from a satellite image) with water level based on the same date basis.

To match flooded areas with water levels, we considered water level during 30 day period prior to the acquisition date of a satellite image, and looked for the peak of water level nearest to the acquisition date. The selected peak might not be the highest value in the 30 day period, but had to be the nearest one. Also, the selected peak must be higher than the lowest point of the river bank. For example, in Figure 6, acquisition date of a satellite image is October, 11, and the nearest water level peak occurred on October, 10. Therefore, flooded areas interpreted from this satellite image were matched with water level of 4.84 m MSL measured on October, 10.

Matching between flooded areas (interpreted from a satellite image) and a water level was processed separately for each influence area. The water level was stored as an attribute of a flood

boundary polygon, and this attribute data showed surface elevation of the flood water. In this study, the flooded areas were multi-date data, and all of them were matched with water levels. When these flooded area polygons were overlaid, contour lines of flood water elevation were illustrated. These contour lines had unequal interval due to different water levels matched, as shown in Figure 7.

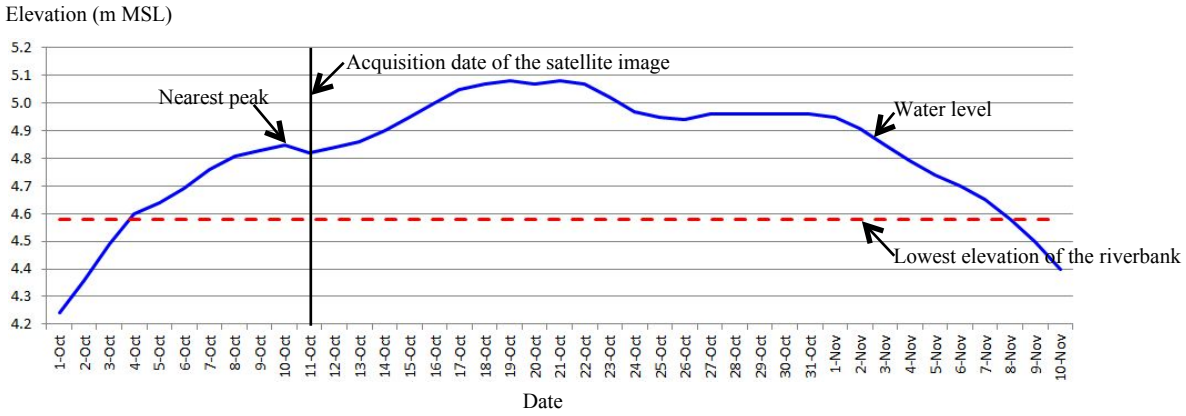

Figure 6 Matching of satellite image acquisition date and water level

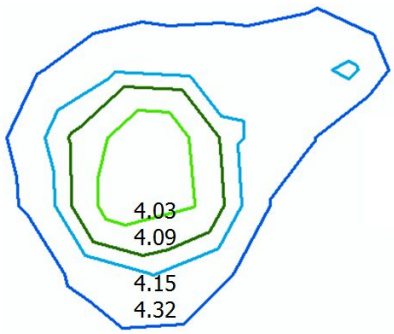

Figure 7 Contour lines of flood water with unequal interval

Each influence area had its own flood water contour line dataset. For flood boundaries interpreted from a same satellite image, if they were in different influence areas, values of flood water elevation (an attribute of the contour line) might be different because water level measured at different gauges might not equal. Furthermore, matching between flooded areas and water levels might yield different peak values.

2.3.3 Water Level Interpolation

Originally, contour interval of the flood water was unequal, as shown in Figure 7. To make the interval equal, spatial interpolation was applied. To retain values of the original data, only exact interpolators were considered, including Inverse Distance Weighting (IDW), Radial Basis Function (RBF), and Kriging. In this study, RBF and Kriging were eliminated because the former yields output values out of range of minimum and maximum of input data, while the later has advantage on directional interpolation, which the overbank flood on a flat terrain like this study does not has obvious directional influence. Hence, IDW was selected. IDW was deemed the most practical method for this study because it is an exact interpolator, yields output values falling within the range of input data, and requires less processing time.

For interpolation of flood water elevation, input data were vertices of the contour lines. Using lines or polygons as the inputs was considered not practical because the elevation values were stored at the centroids, and the elevation values were spatially sparse. In this study, elevation

points were obtained from vertices of the flood water contour lines derived from flood boundaries interpreted from 34 satellite images. The elevation points were dense and suitable for describing variation of flood water surface elevation in the study area.

Output from the interpolation was a surface portraying spatial variation of flood water surface elevation of each influence area. The 3 surfaces of 3 influence areas were then transformed to contour lines with 10 cm interval complying with interval of the LiDAR DEM. These contour lines were later used in the creation of LUT.

2.3.4 Flood Water Depth Calculation

Apart from predicted flooded areas, the developed model also provided the flood water depth surface as another output. Flood depth surface was available only in the boundary of predicted flooded areas. For every polygon of the flooded areas, there was an attribute storing elevation of flood water obtained from the interpolation in the previous step. Flood water depth was calculated from the subtraction of topographic elevation from flood water elevation.

The flood depth surface was in raster format created based on the LiDAR DEM. As a result, the flood water depths stepped up or down 10 cm each time according to the DEM. Water levels measured at the gauges were in cm unit, but interval of the flood depth was 10 cm. For that reason, the model might give the same flood water depth surface for water levels those were few cm different. For example, when flood water elevations were 2.11 and 2.14 m, the model gave the same flood water depth surface based on the flood water elevation of 2.10 m MSL because both 2.11 and 2.14 were rounded down to 2.10.

2.3.5 LUT Creation

To develop the flood model, 3 basic rules were set as follows:

(1) There is no flood in an influence area if the user inputs a water level (at a gauge station) that is lower than the lowest point of the river bank, or lower than the lowest water level matched with historic flooded areas (interpreted from the satellite images).

(2) If the user inputs a water level that can be matched with flooded areas interpreted form the satellite images, predicted flooded areas will be prepared as stated in item 2.3.2 and 2.3.3.

(3) If the user inputs a water level that is higher than the lowest point of the river bank, and also higher than maximum of water level matched with historic flooded areas interpreted from the satellite images (that means no historical flood that the flood water is so this high), predicted flooded areas are generated flooded areas. To generate flooded areas for this case, the LiDAR DEM and the available satellite images were utilized. First, flooded areas matched with the highest water level in the record were used as a base. Next, DEM pixels with elevation equal or lower than the water level input by the user were selected because these pixels were considered flooded. Finally, the base and the selected flooded DEM pixels were combined, and then the generated flooded areas for this case were derived.

Based on these rules, we created LUT containing 3 fields: water level, flooded area, and flood depth, as shown in Table 1. There were 3 LUTs according to the 3 influence areas. To access data in the LUTs, the primary key was water level input by the user.

3. Results

The developed flood model using high resolution DEM, hydrological data and satellite images incorporated techniques to delineate influence areas of the gauge stations, matching between flooded areas and water levels, water level interpolation, flood water depth calculation, and LUT creation. The developed model was implemented using Python language. File size of the created LUT, flooded areas, and flood depths was approximately 85 GB covering the 865 sq. km study area.

Inputs of the model were predicted water levels of 3 gauge stations, including S.5, C.29, and C.35. These 3 days in advance predicted data are provided by the Royal Irrigation Department available during critical periods. There were 2 options for inputting the data including (a) input 1 day

data, and (b) input 3 day data, as shown in Figure 8 (a) and (b) respectively. If the predicted water level was not available, zero was a default value.

Table 1 Structure of LUT

Water level (m MSL)	Flooded areas	Flood depth
water level <= lowest point of the river bank or water level < lowest water level matched with historic flooded areas	no flood	no depth
water level > lowest point of the river bank and water level is between min and max of interpolated flood water elevation	link to a shape file location (interpolated flooded areas)	link to a raster file showing flood depth
water level > lowest point of the river bank and water level > max of interpolated flood water elevation	link to a shape file location (generated flooded areas)	link to a raster file showing flood depth

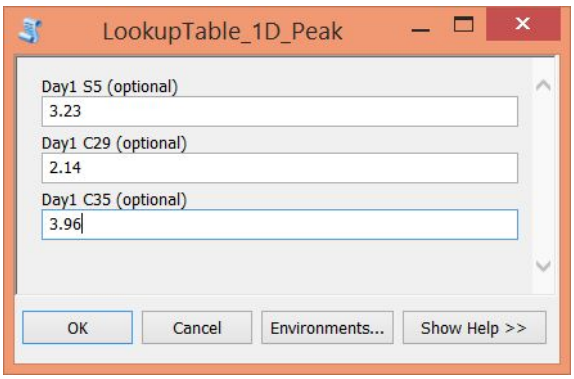

(a)

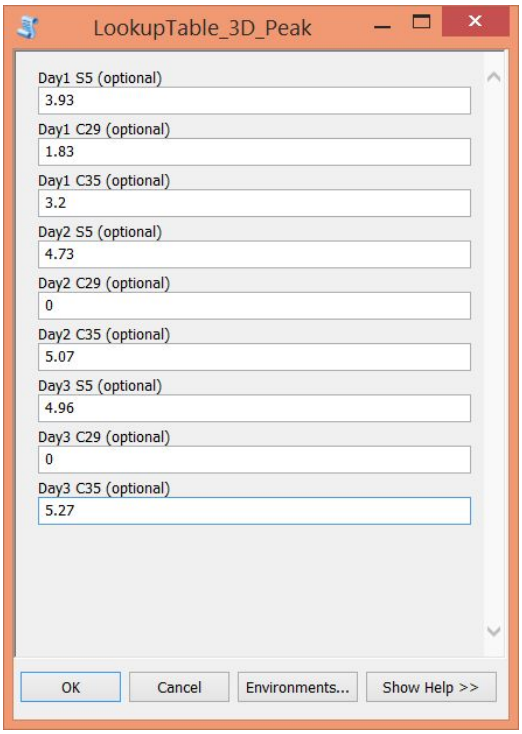

(b)

Figure 8 Options for data inputting (a) 1 day, and (b) 3 days

According to Figure 8 (a), input data of the 3 gauges are S.5=3.23, C.29=2.14, and C.35=3.96 m MSL, and the outputs including predicted flooded areas, and flood water depths are illustrated in Figure 9 and 10 respectively. These outputs were accessed through the LUT.

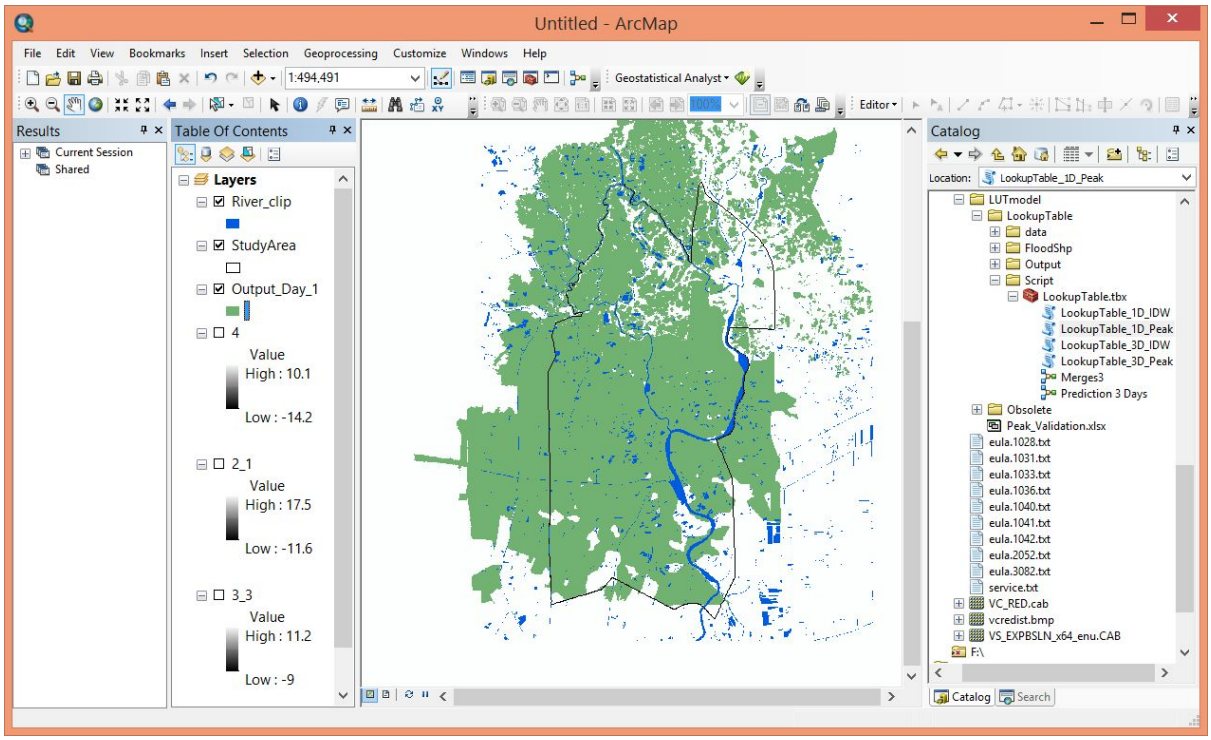

Figure 9 Predicted flooded areas when water level of S.5=3.23, C.29=2.14, and C.35=3.96 m MSL

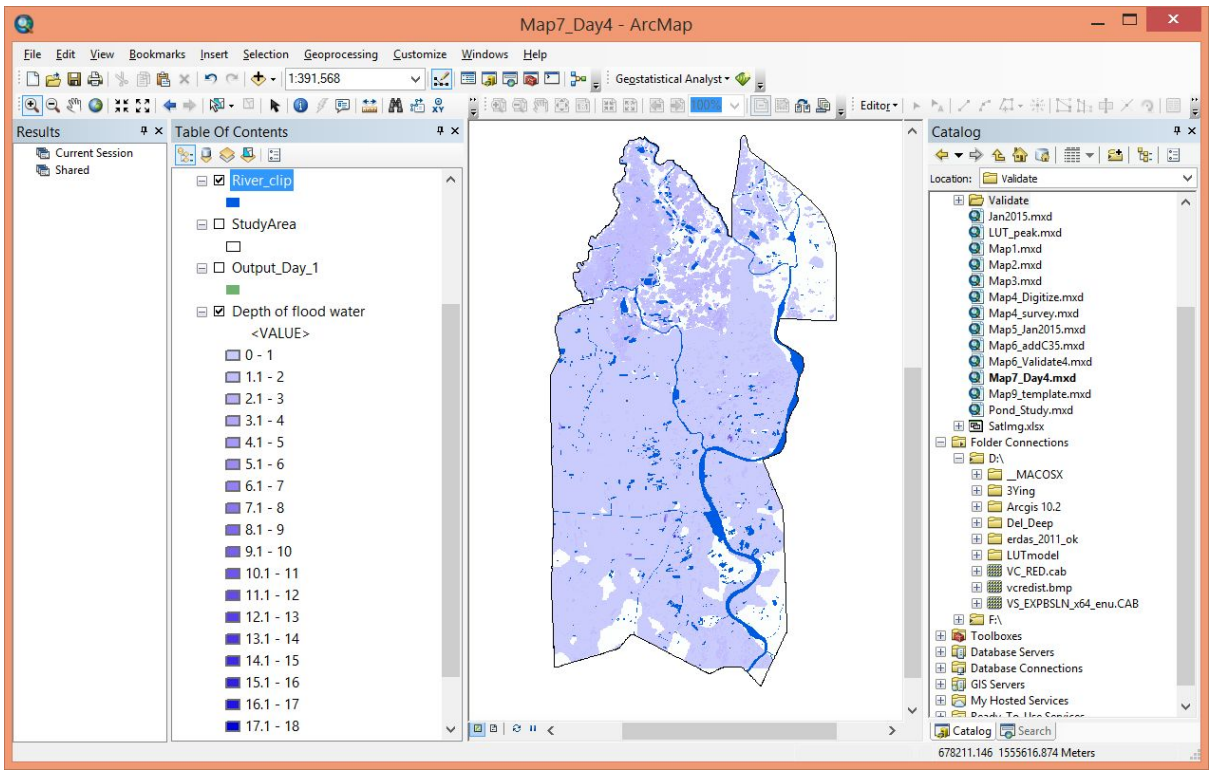

Figure 10 Predicted flood depths when water level of S.5=3.23, C.29=2.14, and C.35=3.96 m MSL

4. Conclusion

The developed flood model using high resolution DEM, hydrological data and satellite images required predicted water levels of C.35, S.5, and C.29 stream gauge stations as inputs, and rapidly yielded outputs as predicted flooded areas and flood depths. The developed flood prediction method is suitable for flood prone areas with sparse gauges, cross sections or other factors required in other flood models.

Accuracy of the model depends on input data (predicted water levels) and historical flooded areas interpreted from satellite images. Among the 3 stream gauge stations, C.29 influenced more than half of the study area. Thus, data continuity and prediction accuracy at this station is important for flood prediction in the study area.

In this study, only 3 gauges were used. If more gauges are set up in the study area, variation of flood water level will be clearly described. As a result, for further study, we plan to set up more gauges in this area and establish mathematical relationship between water levels and flooded areas interpreted from satellite images.

5. References

Arnesen, A. S., Silva, T. S.F., Hess, L. L., Novo, E. M.L.M., Rudorff, C. M., Chapman, B. D., and McDonald, K. C. (2013). Monitoring flood extent in the lower Amazon River floodplain using ALOS/PALSAR ScanSAR images. *Remote Sensing of Environment*, 130, 51-61.

ESRI. (2014). ArcGIS Desktop Help 10.2, 10.2.1, and 10.2.2 – Performing cross-validation and validation. ONLINE. Available: http://resources.arcgis.com/en/help/main/10.2/index.html#//003100000059000000, 3/16/2015.

Marti-Cardona, B., Lopez-Martinez, C., Dolz-Ripolles, J., and Blad-Castellet, E. (2010). ASAR polarimetric, multi-incidence angle and multitemporal characterization of Donana wetlands for flood extent monitoring. *Remote Sensing of Environment*, 114, 2802-2815.

Mason, D.C., Schumann, G.J.-P., Neal, J.C., Garcia-Pintado, J. and Bates, P.D. (2012). Automatic near real-time selection of flood water levels from high resolution Synthetic Aperture Radar images for assimilation into hydraulic models: A case study. *Remote Sensing of Environment*, 124, 705-716.

Pulvirenti, L., Chini, M., Pierdicca, N., Guerriero, L., and Ferrazzoli, P. (2011). Flood monitoring using multi-temporal COSMO-SkyMed data: Image segmentation and signature interpretation. *Remote Sensing of Environment*, 115, 990-1002.

Schumann, G. J.-P., Neal, J. C., Mason, D. C., and Bates, P. D. (2011). The accuracy of sequential aerial photography and SAR data for observing urban flood dynamics, a case study of the UK summer 2007 floods. *Remote Sensing of Environment*, 115, 2536-2546.